Filopodium retraction is controlled by adhesion to its tip

Stephane Romero[1,2,3,4,*], Alessia Quatela[5,*], Thomas Bornschlögl[5,*], Stéphanie Guadagnini[6], Patricia Bassereau[5,‡] and Guy Tran Van Nhieu[1,2,3,4,‡]

[1]Equipe Communication Intercellulaire et Infections Microbiennes, Centre de Recherche Interdisciplinaire en Biologie (CIRB), Collège de France, Paris, France
[2]Institut National de la Santé et de la Recherche Médicale (Inserm) U1050, Paris, France
[3]Centre National de la Recherche Scientifique (CNRS), UMR7241, Paris, France
[4]MEMOLIFE Laboratory of Excellence and Paris Science Lettre, Paris, France
[5]Institut Curie, Centre de Recherche, CNRS, UMR 168, Physico-Chimie Curie, Université Pierre et Marie Curie, F-75248 Paris, France
[6]Plate-forme de Microscopie Ultrastructurale, Institut Pasteur, Paris, France

*These authors contributed equally to this work
‡Authors for correspondence (patricia.bassereau@curie.fr; guy.tran-van-nhieu@college-de-france.fr)

Journal of Cell Science 125, 5587

doi: 10.1242/jcs.126540

There was an error published in *J. Cell Sci.* **125**, 4999-5004.

The name of the third author, Thomas Bornschlögl, was incorrectly given as Thomas Bornschlög. The correct header is as shown above.

We apologise for this mistake.

Filopodium retraction is controlled by adhesion to its tip

Stephane Romero[1,2,3,4,*], Alessia Quatela[5,*], Thomas Bornschlög[5,*], Stéphanie Guadagnini[6], Patricia Bassereau[5,‡] and Guy Tran Van Nhieu[1,2,3,4,‡]

[1]Equipe Communication Intercellulaire et Infections Microbiennes, Centre de Recherche Interdisciplinaire en Biologie (CIRB), Collège de France, Paris, France
[2]Institut National de la Santé et de la Recherche Médicale (Inserm) U1050, Paris, France
[3]Centre National de la Recherche Scientifique (CNRS), UMR7241, Paris, France
[4]MEMOLIFE Laboratory of Excellence and Paris Science Lettre, Paris, France
[5]Institut Curie, Centre de Recherche, CNRS, UMR 168, Physico-Chimie Curie, Université Pierre et Marie Curie, F-75248 Paris, France
[6]Plate-forme de Microscopie Ultrastructurale, Institut Pasteur, Paris, France

*These authors contributed equally to this work
‡Authors for correspondence (patricia.bassereau@curie.fr; guy.tran-van-nhieu@college-de-france.fr)

Accepted 29 June 2012
Journal of Cell Science 125, 4999–5004

doi: 10.1242/jcs.104778

Summary

Filopodia are thin cell extensions sensing the environment. They play an essential role during cell migration, cell–cell or cell–matrix adhesion, by initiating contacts and conveying signals to the cell cortex. Pathogenic microorganisms can hijack filopodia to invade cells by inducing their retraction towards the cell body. Because their dynamics depend on a discrete number of actin filaments, filopodia provide a model of choice to study elementary events linked to adhesion and downstream signalling. However, the determinants controlling filopodial sensing are not well characterized. In this study, we used beads functionalized with different ligands that triggered filopodial retraction when in contact with filopodia of epithelial cells. With optical tweezers, we were able to measure forces stalling the retraction of a single filopodium. We found that the filopodial stall force depends on the coating of the bead. Stall forces reached 8 pN for beads coated with the β1 integrin ligand *Yersinia* Invasin, whereas retraction was stopped with a higher force of 15 pN when beads were functionalized with carboxyl groups. In all cases, stall forces increased in relation to the density of ligands contacting filopodial tips and were independent of the optical trap stiffness. Unexpectedly, a discrete and small number of *Shigella* type three secretion systems induced stall forces of 10 pN. These results suggest that the number of receptor–ligand interactions at the filopodial tip determines the maximal retraction force exerted by filopodia but a discrete number of clustered receptors is sufficient to induce high retraction stall forces.

Key words: Filopodia, Force measurements, Optical tweezers, Adhesion

Introduction

Filopodia are thin cell extensions containing actin filaments, acting as pathfinders during cell migration or neuronal guidance and controlling initial steps of cell adhesion (Rørth, 2003; Small and Resch, 2005). Several bacteria or viruses also hijack filopodia to invade epithelial or endothelial cells (Lehmann et al., 2005; Romero et al., 2011; Schelhaas et al., 2008; Smith et al., 2008; Young et al., 1992). For example, the *Yersinia* Invasin protein that binds to β1 integrins and the *Shigella* Type III Secretion System (T3SS) have been shown to interact with and trigger retraction of filopodia (Romero et al., 2011; Vonna et al., 2007; Young et al., 1992). While forces exerted during cell adhesion or migration have been analysed in many studies, forces associated with filopodia have been characterized in only a few systems (Howard, 2001; Kress et al., 2007; Moore et al., 2010; Vonna et al., 2007). Filopodia generate pushing forces of a few pN during their elongation (Cojoc et al., 2007), consistent with pushing forces exerted by polymerizing actin of typically 1 pN per filament (Footer et al., 2007; Mogilner and Rubinstein, 2005). In filopodia, actin filaments are organized in parallel bundles by cross-linking and bundling proteins with their barbed ends towards the filopodial tip (Mallavarapu and Mitchison, 1999; Vignjevic et al., 2006). Actin nucleation directed at plasma membrane sites and filament elongation at their barbed ends control filopodia formation and growth (Faix and Rottner, 2006; Gupton and Gertler, 2010). The molecular mechanisms controlling retraction are less understood. Current retraction models involve the retrograde flow of filopodial actin filaments, which is not compensated by actin assembly at the filopodial tip (Mallavarapu and Mitchison, 1999). Myosin-II, anchored to the actin cortical network, may participate in the retrograde flow but is unlikely to represent the only mechanism since in macrophage, filopodia still retract in the presence of blebbistatin (Kress et al., 2007).

While filopodia interact with various substrates, including cadherins or extracellular matrix components (Partridge and Marcantonio, 2006; Vasioukhin et al., 2000), little is known about the effects of these interactions on filopodial properties. Here, we have analyzed the role of contact properties on retraction forces associated with a single filopodium interacting at its tip with ligand-functionalized beads. For this, we used optical tweezers (OTs) to exert a counterforce. We found that for all tested ligands, contact with the filopodial tip triggered filopodial retraction and that the maximal retraction force depended on the density of ligands presented to the filopodial tips.

Results and Discussion

The density of β1 integrin ligands presented at the tip of filopodia controls filopodial retraction

To measure the force applied by the retraction of a single filopodium, we used a set up combining fluorescence confocal microscopy and OTs (Sorre et al., 2009). This set up allowed us to visualize the number of filopodia interacting with the beads while performing force measurements (Fig. 1A). Briefly, prior to acquisition cells labelled with a fluorescent membrane dye were incubated with beads. We first used as a bead coating ligand the *Yersinia* Invasin protein, which specifically binds to β1 integrins and triggers filopodial retraction (Young et al., 1992; Isberg and Barnes, 2001; Vonna et al., 2007). A bead was immobilized in the OTs and approached to a single filopodium emanating from the cell (Fig. 1B). The bead motion in the trap was recorded by video microscopy, while monitoring filopodium retraction by confocal microscopy. The force F applied by the OTs was calculated from the bead position. This force F increases as a function of the bead displacement Δx away from the trap centre and is given by $F = k_x \Delta x$, where k_x is the trap stiffness that depends on the laser power (Neuman and Block, 2004). At the end of the experiment, z-stack acquisitions were performed to visualize all filopodia interacting with the bead (Fig. 1C).

As shown in Fig. 1D, Invasin-coated beads were observed to trigger filopodial retraction. At a trap stiffness of 54 pN/μm, after a lag phase, the bead was pulled by the retracting filopodium (Fig. 1D, left panel, blue curve) and reached an equilibrium position where the force exerted by the retracting filopodium was counteracted by the force exerted by the OTs, referred to as the 'stall force' (Fig. 1D, right panel, white dashed line). When force measurements were performed at 80 pN/μm, a similar stall force was observed, indicating that the trap stiffness had no effects on the stall force (Fig. 1D, red curve). Often, other filopodia were observed to contact the bead as it approached the cell, leading to

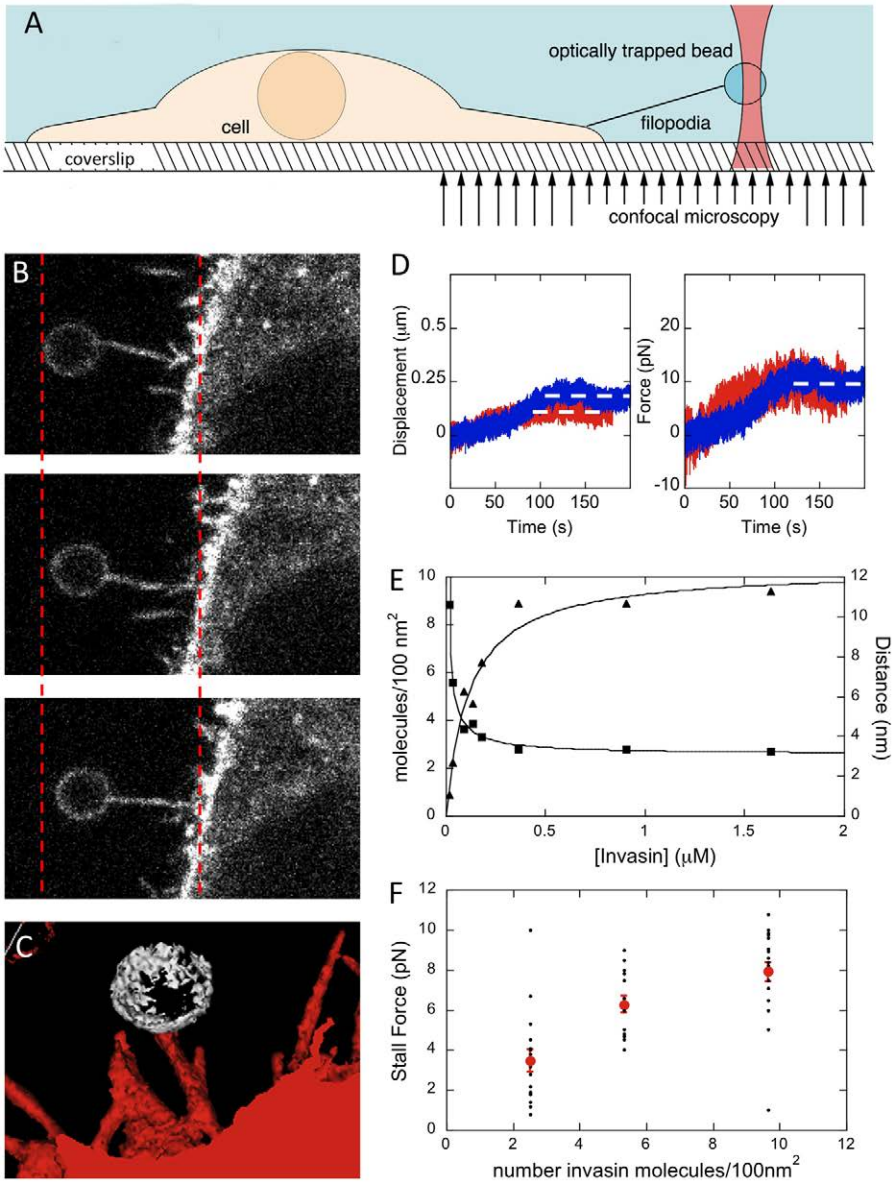

Fig. 1. Force measurement associated with the retraction of a single filopodium. (**A**) Schematic representation of the experimental setup. Invasin-coated beads were immobilized in the OTs and brought in contact with the tip of a single filopodium. The plasma membrane was stained with the fluorescent dye FM4-64. (**B**) Confocal images were acquired to monitor filopodial interaction with the bead during retraction. (**C**) 3D reconstruction from a z-stack at the end of the experiment showing a single filopodium interacting with the bead. (**D**) The position of the bead (left panel) was derived from video recording at 30 Hz to calculate the force applied by the OTs, for a trap stiffness of 54 (blue) or 80 (red) pN/μm. The bead moved until the force exerted by the OTs counteracted the force exerted by the filopodium (right panel), corresponding to the stall force (dashed lines). (**E**) The calculated density of Invasin molecules per 100 nm^2 on the bead surface (triangles) or the average distance between two molecules (squares) expressed as a function of the Invasin bulk concentration and can be accounted for as a standard hyperbolic saturation curve. (**F**) The retraction force exerted by a single filopodium, recorded at k_x, ranging between 42 and 80 pN/μm, depends on the density of Invasin on the bead. Individual stall force measurements (black circles) and the mean of the stall force (red circles) is represented (±s.e.m.) as a function of the number of Invasin molecules per 100 nm^2.

high stall forces (supplementary material Fig. S1). In such cases, the experiments were discarded from the analysis and only those involving retraction of a single filopodium were considered.

We next investigated whether the density of Invasin on the bead interacting with β1 integrins present at the filopodial tip could affect the stall force. Beads were first incubated with purified recombinant Invasin at concentrations ranging from 18 nM to 1.6 μM, then passivated with BSA. The number of immobilized Invasin was calculated from quantitative western blot analysis and showed that saturation occurred at 9.6 Invasin molecules adsorbed per 100 nm^2, corresponding to a distance of 3.2 nm between two molecules (Fig. 1E) At a partial coating bulk concentration of 40 nM, 2.2 Invasin molecules were adsorbed per 100 nm^2 corresponding to a distance of 6.7 nm between two molecules (Materials and Methods; Fig. 1E).

Fig. 1F shows the stall force, recorded at trap stiffness ranging from 42 to 80 pN/μm, plotted as a function of the number of immobilized Invasin molecules for each coating condition. The stall force associated with filopodial retraction decreased from 7.9±0.9 to 3.4±0.6 pN as the number of Invasin molecules per 100 nm^2 decreased from 9.6 to 2.2, respectively (Fig. 1F, 51 determinations, 13 independent experiments). Under these Invasin partial coating conditions, bead detachment from the filopodial tip was occasionally observed. Such detachment was never observed in all other conditions used. These results indicate that the density of Invasin on beads bound to the filopodial tip is a critical parameter that controls the force associated with filopodial retraction.

The density of adhesive links on the bead determines the stall force associated with filopodial retraction

Beads with different surface properties were tested for filopodial capture and retraction using time-lapse phase contrast microscopy. We found that highly charged hydrophilic polystyrene beads functionalized with anionic carboxyl groups (supplementary material Fig. S2A) or cationic amine groups, as well as glass beads, bound to filopodia and triggered their retraction (data not shown). In contrast, filopodial interaction did not occur when carboxylated beads were saturated with BSA (supplementary material Fig. S2B; 19 cells, three independent

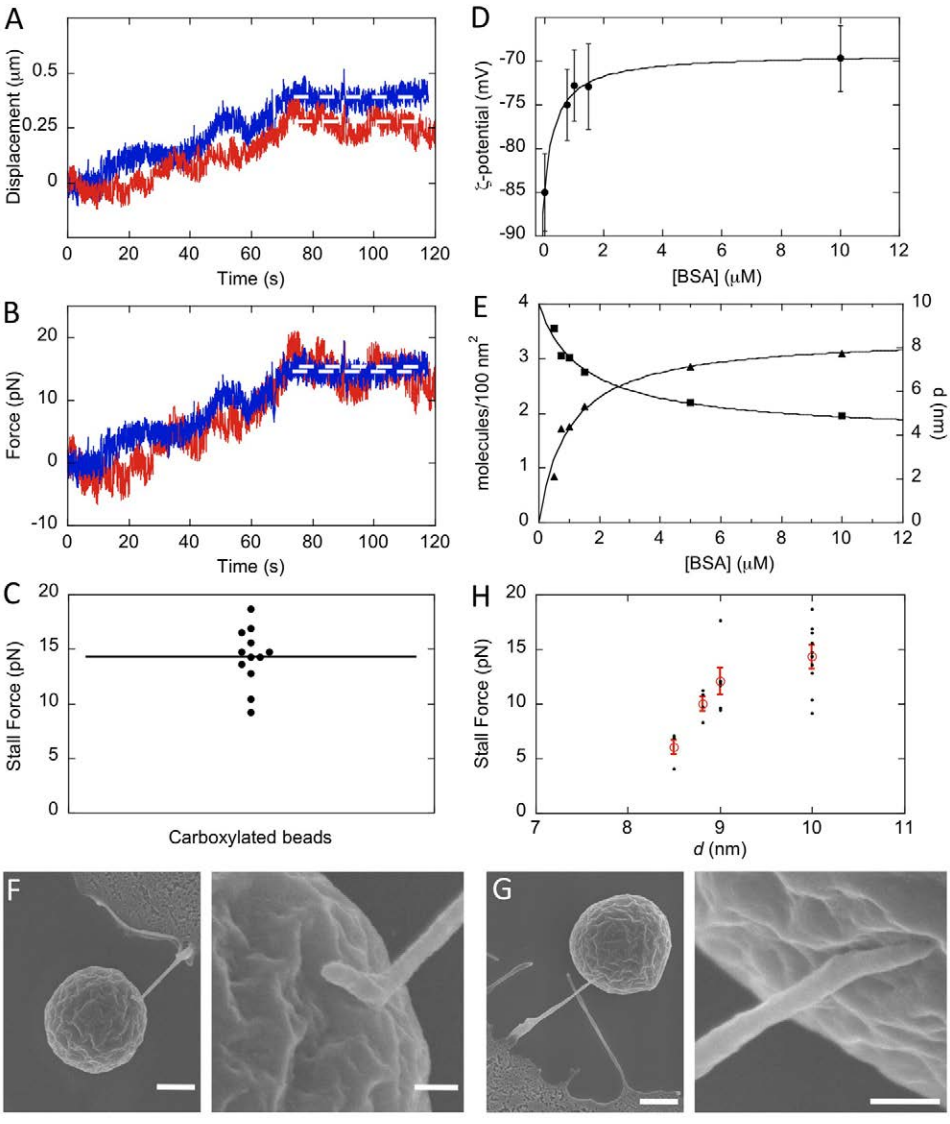

Fig. 2. The filopodial retraction stall force depends on the density of reactive groups on the bead surface. (**A**,**B**) Plots of the displacement of carboxylated beads (A), or of the force applied by the OTs on beads (B) versus time. Trap stiffness: 42 pN/μm (blue) or 55 pN/μm (red). White dashed lines: stall force position. (**C**) Stall forces related to filopodial retraction were determined for carboxylated beads (12 determinations, 10 independent experiments) at different trap stiffnesses. The mean is represented by a horizontal line. (**D**) Zeta-potential of the carboxylated beads (0.25% solids in B buffer) as a function of BSA concentrations of the incubation solutions. (**E**) Characterization of the density of BSA on the bead surface. Triangles and squares represent the density of BSA molecules per 100 nm^2 and the square root of the uncoated surface per 100 nm^2, *d*, respectively. (**F**,**G**) Scanning electron micrographs of carboxylated beads, uncoated (F) or coated with 1.5 μM of BSA (G), captured by filopodia (left panels; scale bars: 1000 nm). Right panels show enlargements of filopodial–bead interaction (scale bars: 200 nm). (**H**) The stall force of a single filopodium, recorded at k_x ranging between 42 and 80 pN/μm, depends on the density of interacting sites between filopodial tips and partially BSA-coated beads. Individual stall force measurements (black circles) and the mean of the stall force(red circles; ± s.e.m.) are plotted as a function of *d*.

experiments). The adhesive properties of the beads were further tested by forcing contact with filopodia at the cell periphery or the cell cortex using OTs (Material and Methods).

We next measured the stall force of single filopodia using carboxylated beads. This stall force averaged 14.3±0.7 pN, a value significantly higher than that measured for Invasin-coated beads (Fig. 2C, 12 determinations, 10 independent experiments, $P<0.001$). As for Invasin-coated beads, we did not observe a change in the stall force using different trap stiffness of $k_x=42$ or 55 pN/µm (Fig. 2A,B). To investigate whether the density of adhesive links between the filopodia and the bead affected the stall force, beads were coated with BSA to reduce adhesion to the filopodium. Carboxylated beads were incubated with BSA solutions ranging from 0 to 10 µM. Zeta-potential measurements showed that the absolute charge of carboxylated beads decreased with BSA coating and plateaued when beads were incubated in 10 µM BSA solution (Fig. 2D), consistent with the blocking of negatively charged carboxyl groups. In parallel experiments, BSA was stripped from the beads and subjected to quantitative Coomassie-staining SDS-PAGE. From this analysis, the number of BSA molecules adsorbed per 100 nm^2 of bead surface was calculated and d, the square root of the free surface was plotted as a function of the BSA bulk concentration (Fig. 2E). Thus d reflects the number of potential interacting sites with the filopodial tip. Scanning electron microscopy analysis showed that partial coating of beads with BSA did not prevent their binding to filopodia (Fig. 2F), and that the bead area in contact with filopodia did not significantly differ from that of uncoated carboxylated beads (ca. 27,500–32,000 nm^2, two independent experiments, more than six determinations; Fig. 2G). Beads coated with various BSA concentrations were then used for force measurements. Fig. 2H shows the stall force plotted as a function of d for each coating conditions. As d increased, the stall force associated with the retracting filopodia increased from 6±0.6 pN to 14.3±0.7 pN, this highest value corresponding to uncoated carboxylated beads. These results confirm that the density of adhesive bonds between the filopodial tip and the beads controls the stall force exerted by a filopodium.

Modelling filopodial retraction induced by the *Shigella* T3SS interaction

We have previously shown that the presence of the T3SS at the surface of *Shigella* is required to trigger filopodial retraction (Romero et al., 2011). Polystyrene beads coated with purified membranes from wild-type *Shigella* containing the T3SS also interacted with filopodia and triggered their retraction within a few seconds, in a process similar to that observed with *Shigella* (supplementary material Fig. S2C,D; Movie 1). Beads coated with membranes purified from a T3SS-defective *Shigella mxiD* mutant did not induce retraction, suggesting that as for bacteria, the T3SS is required for binding to filopodia (supplementary material Fig. S2E; Movie 2, three independent experiments, 27 cells) (Romero et al., 2011). The analysis of beads and bacteria trajectories showed that the maximum velocity of filopodial retraction did not significantly differ between functionalized beads and bacteria, with speeds ranging from 1.7±0.3 to 2.5±0.3 µm/min (supplementary material Fig. S2G).

When trapped into OTs, wild-type *Shigella*-membrane-coated beads consistently attached to filopodia and induced retraction (data not shown). As illustrated in Fig. 3A,B, measurements at $k_x=24$ or 60 pN/µm resulted in a similar stall force,

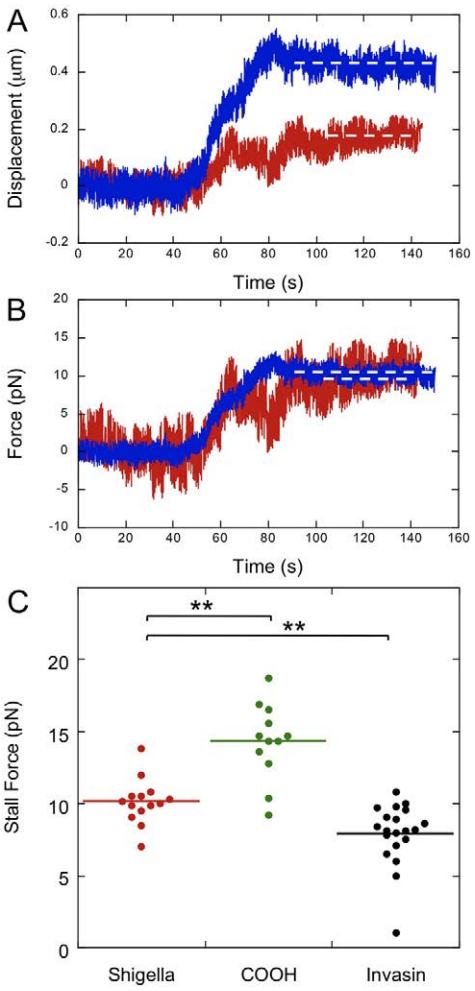

Fig. 3. The stall force of a single retracting filopodium differs for beads coated with *Shigella*-membranes and carboxylated beads. (**A**,**B**) Plots of the displacement of *Shigella*-membrane-coated beads (A), or of the force applied by the OTs on beads (B) versus time. Trap stiffness: 24 pN/µm (blue) or 60 pN/µm (red). White dashed lines: stall force position. (**C**) Stall forces associated with filopodial retraction, recorded at k_x ranging between 24 and 80 pN/µm, were determined for beads functionalized with *Shigella* membranes (red; 14 determinations, 12 independent experiments), carboxyl groups (green; 12 determinations, 10 independent experiments) or Invasin at saturation (black; 20 determinations, 13 independent experiments). Horizontal lines represents the mean stall force. **$P<0.001$.

corresponding to a mean value of 10.1±1.5 pN (Fig. 3C; 14 determinations, 12 independent experiments).

We found in this study that adhesion of beads coated with different ligands to the tip of filopodia induced their retraction, which can be stalled by forces depending on the nature and number of adhesive links between beads and the filopodial tip. We estimated that beads coated with Invasin molecules, spaced at an average distance of 7 or 3 nm, led to 3 or 8 pN stall forces, respectively. This is consistent with the observation in another system, that the distance between β1 integrin ligands controls cell adhesion (Fig. 4A) (Selhuber-Unkel et al., 2008). Interestingly, beads coated with T3SS-containing *Shigella* membranes induced a filopodial stall force of 10 pN. Because of the limited number of T3SS at the surface of *Shigella* (Blocker et al., 1999), only one

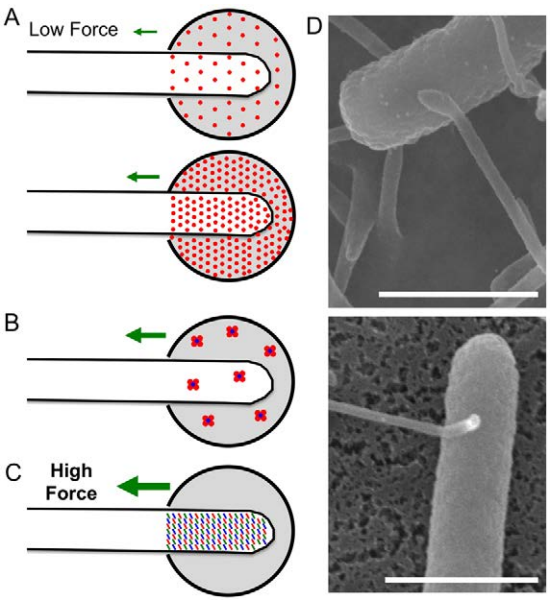

Fig. 4. Filopodial retraction stall force is controlled by ligand clustering. (**A**) Signalling induced by a low density of Invasin (red dots) on the bead induces filopodial retraction that is stalled with a lower force (top panel) than by a high Invasin density (bottom panel). (**B**) When the filopodium interacts with the T3SS (red and blue clusters), a few clusters of ligands are sufficient to induce retraction with a higher stall force than at a high density of Invasin molecules. (**C**) Carboxylated beads interacting with different types of receptors, depicted by multi-coloured rectangles, induce filopodial retraction with a high stall force. The width of the green arrows represents the strength of the stall force; empty finger-like shapes represent filopodia; grey circles represent the beads. (**D**) Scanning electron micrographs of *Shigella* interacting with filopodia. The filopodial area contacting the bacterium does not significantly differ from that contacting the beads (Materials and Methods). Scale bar: 1 µm.

or two T3SS present in bacterial membranes coating the surface of the bead may interact with filopodia (Materials and Methods). The T3SS tip complex proteins IpaB and IpaD, required for filopodial interaction, have been proposed to form a pentamer (Veenendaal et al., 2007; Romero et al., 2011). Our results suggest that clustering of a few receptors caused by a discrete number of pentameric T3SS tip complexes is sufficient to induce filopodial retraction with at least a similar stall force than a much larger number of Invasin molecules, uniformly distributed over the bead surface (Fig. 4B). Moreover, for the T3SS, interaction with a combination of different receptors could also result in a higher stall force than with a single family of receptors as in the case of β1-integrin–Invasin binding. As for Invasin-coated beads, the binding of carboxylated beads to filopodia or the cell cortex was reduced by the Ca^{2+} chelator EGTA, consistent with the implication of Ca^{2+}-dependent receptors such as integrins (supplementary material Fig. S3A) (Leitinger et al., 2000). In addition to the α5β1 integrin, however, recruitment of E-cadherin could also be detected at the filopodial contact site with carboxylated beads (supplementary material Fig. S3B). These results suggest that in the case of carboxylated beads, interaction with multiple types of receptors can induce stall forces of up to 15 pN (Fig. 4C).

There are at least two possible origins for the dependence of retraction stall force on the ligand density. The ligand density, possibly through receptor clustering, could determine the number of receptors at the filopodial tip, directly or indirectly tethered to internal actin filaments. The arrest of filopodial retraction at a force applied by OTs could result from a rupture of these links from actin filaments. Alternatively, the ligand density could regulate downstream signalling and modulate actin dynamics or the total number of molecular motors involved in filopodial retraction. Consistent with Kress et al., we found that filopodial retraction was not prevented by blebbistatin, a myosin II inhibitor (Kress et al., 2007; Romero et al., 2011; data not shown). In future works, it will be interesting to study if and how, in response to signalling through distinct receptors, a common machinery implicating myosins other than myosin II, or actin polymerization/depolymerisation is involved to retract filopodia.

Materials and Methods

Plasmid, reagents, cell lines and bacterial strains

The recombinant Invasin expressing plasmid was generated by PCR amplification of the 489–986 cell-binding domain of the *Yersinia* Invasin, and cloned into the pET-101/D-TOPO (Invitrogen). BSA was purchased from Sigma (no. A4503). HeLa cells were obtained from the American Type Culture Collection. Cells were grown in RPMI medium (Gibco) containing 10% foetal calf serum (FCS, Gibco) at 37℃ in a 5% CO_2 incubator. The invasive wild-type *Shigella* M90T and the *mxiD* mutant strains were described previously (Blocker et al., 1999). Bacterial strains were grown in trypticase soy (TCS) broth at 37℃ with agitation.

Bacterial membrane purification

Shigella membranes were purified as described (Robichon et al., 2005). M90T or *mxiD Shigella* strains were grown until OD_{600}=0.8, lysed in a French press, and centrifuged at 3000 rpm to remove cell debris. Supernatants were centrifuged at 48,000 rpm in a 50Ti rotor for 60 min, and pellets were resuspended in 25 mM HEPES buffer pH 7.4. Sucrose crystals were added until saturation (about 60%, checked with a refractometer), samples were deposited at the bottom of an ultracentrifuge tube, overlayed with sucrose solutions ranging from 56 to 36%, and centrifuged for 36 hours in a swinging bucket rotor at 48,000 rpm. 300 µl fractions were collected, and analyzed by anti-OmpC and anti-MxiH western blot (Bernardini et al., 1993; Jouihri et al., 2003). Fractions containing the OmpC and MxiH proteins were pooled and dialyzed against HEPES buffer.

Bead coating and quantification

Carboxylated polystyrene beads (3 µm diameter; Polysciences Inc.; 0.25% suspension) were incubated with purified *Shigella* membranes, or with BSA or Invasin at the indicated concentrations for 1 h at 4℃ in EM buffer (120 mM NaCl, 7 mM KCl, 1.8 mM $CaCl_2$, 0.8 mM $MgCl_2$, 5 mM glucose and 25 mM HEPES at pH 7.3). With the exception of BSA-coated beads which were used subsequently to primary coating, beads were washed and saturated with 1% BSA in EM buffer.

500 µl of the suspension of washed BSA- or Invasin-coated beads were pelleted and denatured in Laemmli loading buffer and analysed by SDS-PAGE followed by quantitative Coomassie staining for BSA-coated beads, or quantitative western blot analysis to determine the amount of immobilized proteins as previously described (Samarin et al., 2003). The number of immobilized molecules per 100 nm^2 was analyzed using the equation:

$$P_{\mathrm{im}} = P_{\mathrm{max}} 100 \frac{K_{\mathrm{d}} P_0}{1 + K_{\mathrm{d}} P_0}, \quad (1)$$

where P_{im} is the amount of immobilized proteins, P_{max} is the maximum number of immobilized molecules per nm^2, K_{d} is the dissociation constant and P_0 is the incubated protein concentration. Data analysis accounted for a K_{d} of 1 and 0.08 mM for BSA and Invasin, respectively.

The distance between two immobilized molecules was analyzed with the equation:

$$D_{\mathrm{im}} = \sqrt{\frac{100}{P_{\mathrm{im}}}}, \quad (2)$$

where D_{im} is the distance between two molecules.

Since D at saturation is 5.6 nm, we considered BSA as a 5.6 nm diameter globular particle, occupying a surface of 25 nm^2. Thus, the square root of the free surface per 100 nm^2, d, was calculated using the equation:

$$d = \sqrt{100 - (P_{\mathrm{im}} S_{\mathrm{BSA}})}, \quad (3)$$

where S_{BSA} is the surface of one BSA molecule.

In ca. 80% of the cases, BSA-saturated beads trapped into OTs did not adhere to cells, when placed in contact with the cell body. In the few remaining cases, when BSA-saturated beads showed cell adhesive properties (Jiang et al., 2003), all beads were discarded and the experiments were not pursued further.

Force measurements

HeLa cells rinsed three times in EM buffer were mounted in a microscope chamber with beads (0.001% suspension) and 1 μM FM4-64 dye (Invitrogen), and put on a 37°C temperature-controlled stage on a NikonTE2000 confocal microscope with a custom-build optical trap, allowing simultaneous confocal and brightfield microscopy, as well as force spectroscopy (Sorre et al., 2009). Free beads were trapped with OTs and brought in contact to filopodial tips. Bead position was then determined by video-tracking of the brightfield image at 30 Hz. The trap stiffness was calibrated using the viscous drag method with a triangular driving force (Neuman and Block, 2004). Note that the noise, e.g. in Fig. 3A, is dominated by the noise from the video tracking method.

Calculation of the filopodial surface in contact with beads and bacteria

The area of filopodia, considered as cylinders, in contact with beads or bacteria was estimated to correspond to one-third of the area of the cylinder and did not statistically differ for beads or bacteria when quantified from SEM micrographs ($P>0.1$). The surface of beads contacting the filopodial tip was estimated to 30,000 nm^2. Between 50 and 100 T3SS have been visualized on the surface of a single bacterium (Blocker et al., 1999). Assuming the bacterium is an ellipsoid of 0.6×2 μm, the surface of a bacterium is 3.7 μm^2 with a density of one T3SS for 37,000 nm^2. Thus, only one or two T3SS are likely to be involved in the interaction with the filopodial tip.

Statistical analysis

Data are reported as means ± s.e.m. (standard error of the mean). An unpaired Student's *t*-test with unequal variance was used, with a *P*-value <0.001 considered significant.

Acknowledgements

The authors thank Pierre Nassoy and Darius Koster-Vasco for help with experiments.

Funding

This work was supported by the Institut National de la Santé et de la Recherche Médicale, Agence Nationale de la Recherche [grant numbers A05142JS and R08056JS to P.B. and G.T.V.N.]; National Institutes of Health [grant number AI067949 to Tina Izard and G.T.V.N.]; Fondation pour la Recherche Médicale [grant number SPF20080512650 to S.R.]; and the Human Frontier Science Program [grant number LT000567/2010-C to T.B.]. Deposited in PMC for release after 12 months.

Supplementary material available online at
http://jcs.biologists.org/lookup/suppl/doi:10.1242/jcs.104778/-/DC1

References

Bernardini, M. L., Sanna, M. G., Fontaine, A. and Sansonetti, P. J. (1993). OmpC is involved in invasion of epithelial cells by Shigella flexneri. *Infect. Immun.* **61**, 3625-3635.

Blocker, A., Gounon, P., Larquet, E., Niebuhr, K., Cabiaux, V., Parsot, C. and Sansonetti, P. (1999). The tripartite type III secreton of Shigella flexneri inserts IpaB and IpaC into host membranes. *J. Cell Biol.* **147**, 683-693.

Cojoc, D., Difato, F., Ferrari, E., Shahapure, R. B., Laishram, J., Righi, M., Di Fabrizio, E. M. and Torre, V. (2007). Properties of the force exerted by filopodia and lamellipodia and the involvement of cytoskeletal components. *PLoS ONE* **2**, e1072.

Faix, J. and Rottner, K. (2006). The making of filopodia. *Curr. Opin. Cell Biol.* **18**, 18-25.

Footer, M. J., Kerssemakers, J. W., Theriot, J. A. and Dogterom, M. (2007). Direct measurement of force generation by actin filament polymerization using an optical trap. *Proc. Natl. Acad. Sci. USA* **104**, 2181-2186.

Gupton, S. L. and Gertler, F. B. (2010). Integrin signaling switches the cytoskeletal and exocytic machinery that drives neuritogenesis. *Dev. Cell* **18**, 725-736.

Howard, J. (2001) *Mechanics of Motor Proteins and the Cytoskeleton*. Sunderland, MA: Sinauer Associates.

Isberg, R. R. and Barnes, P. (2001). Subversion of integrins by enteropathogenic Yersinia. *J. Cell Sci.* **114**, 21-28.

Jiang, G., Giannone, G., Critchley, D. R., Fukumoto, E. and Sheetz, M. P. (2003). Two-piconewton slip bond between fibronectin and the cytoskeleton depends on talin. *Nature* **424**, 334-337.

Jouihri, N., Sory, M. P., Page, A. L., Gounon, P., Parsot, C. and Allaoui, A. (2003). MxiK and MxiN interact with the Spa47 ATPase and are required for transit of the needle components MxiH and MxiI, but not of Ipa proteins, through the type III secretion apparatus of Shigella flexneri. *Mol. Microbiol.* **49**, 755-767.

Kress, H., Stelzer, E. H., Holzer, D., Buss, F., Griffiths, G. and Rohrbach, A. (2007). Filopodia act as phagocytic tentacles and pull with discrete steps and a load-dependent velocity. *Proc. Natl. Acad. Sci. USA* **104**, 11633-11638.

Lehmann, M. J., Sherer, N. M., Marks, C. B., Pypaert, M. and Mothes, W. (2005). Actin- and myosin-driven movement of viruses along filopodia precedes their entry into cells. *J. Cell Biol.* **170**, 317-325.

Leitinger, B., McDowall, A., Stanley, P. and Hogg, N. (2000). The regulation of integrin function by Ca(2+). *Biochim. Biophys. Acta* **1498**, 91-98.

Mallavarapu, A. and Mitchison, T. (1999). Regulated actin cytoskeleton assembly at filopodium tips controls their extension and retraction. *J. Cell Biol.* **146**, 1097-1106.

Mogilner, A. and Rubinstein, B. (2005). The physics of filopodial protrusion. *Biophys. J.* **89**, 782-795.

Moore, S. W., Roca-Cusachs, P. and Sheetz, M. P. (2010). Stretchy proteins on stretchy substrates: the important elements of integrin-mediated rigidity sensing. *Dev. Cell* **19**, 194-206.

Neuman, K. C. and Block, S. M. (2004). Optical trapping. *Rev. Sci. Instrum.* **75**, 2787-2809.

Partridge, M. A. and Marcantonio, E. E. (2006). Initiation of attachment and generation of mature focal adhesions by integrin-containing filopodia in cell spreading. *Mol. Biol. Cell* **17**, 4237-4248.

Robichon, C., Vidal-Ingigliardi, D. and Pugsley, A. P. (2005). Depletion of apolipoprotein N-acyltransferase causes mislocalization of outer membrane lipoproteins in Escherichia coli. *J. Biol. Chem.* **280**, 974-983.

Romero, S., Grompone, G., Carayol, N., Mounier, J., Guadagnini, S., Prevost, M. C., Sansonetti, P. J. and Van Nhieu, G. T. (2011). ATP-mediated Erk1/2 activation stimulates bacterial capture by filopodia, which precedes Shigella invasion of epithelial cells. *Cell Host Microbe* **9**, 508-519.

Rørth, P. (2003). Communication by touch: role of cellular extensions in complex animals. *Cell* **112**, 595-598.

Samarin, S., Romero, S., Kocks, C., Didry, D., Pantaloni, D. and Carlier, M. F. (2003). How VASP enhances actin-based motility. *J. Cell Biol.* **163**, 131-142.

Schelhaas, M., Ewers, H., Rajamäki, M. L., Day, P. M., Schiller, J. T. and Helenius, A. (2008). Human papillomavirus type 16 entry: retrograde cell surface transport along actin-rich protrusions. *PLoS Pathog.* **4**, e1000148.

Selhuber-Unkel, C., López-García, M., Kessler, H. and Spatz, J. P. (2008). Cooperativity in adhesion cluster formation during initial cell adhesion. *Biophys. J.* **95**, 5424-5431.

Skoudy, A., Mounier, J., Aruffo, A., Ohayon, H., Gounon, P., Sansonetti, P. and Tran Van Nhieu, G. (2000). CD44 binds to the Shigella IpaB protein and participates in bacterial invasion of epithelial cells. *Cell. Microbiol.* **2**, 19-33.

Small, J. V. and Resch, G. P. (2005). The comings and goings of actin: coupling protrusion and retraction in cell motility. *Curr. Opin. Cell Biol.* **17**, 517-523.

Smith, J. L., Lidke, D. S. and Ozbun, M. A. (2008). Virus activated filopodia promote human papillomavirus type 31 uptake from the extracellular matrix. *Virology* **381**, 16-21.

Sorre, B., Callan-Jones, A., Manneville, J. B., Nassoy, P., Joanny, J. F., Prost, J., Goud, B. and Bassereau, P. (2009). Curvature-driven lipid sorting needs proximity to a demixing point and is aided by proteins. *Proc. Natl. Acad. Sci. USA* **106**, 5622-5626.

Vasioukhin, V., Bauer, C., Yin, M. and Fuchs, E. (2000). Directed actin polymerization is the driving force for epithelial cell-cell adhesion. *Cell* **100**, 209-219.

Veenendaal, A. K., Hodgkinson, J. L., Schwarzer, L., Stabat, D., Zenk, S. F. and Blocker, A. J. (2007). The type III secretion system needle tip complex mediates host cell sensing and translocon insertion. *Mol. Microbiol.* **63**, 1719-1730.

Vignjevic, D., Kojima, S., Aratyn, Y., Danciu, O., Svitkina, T. and Borisy, G. G. (2006). Role of fascin in filopodial protrusion. *J. Cell Biol.* **174**, 863-875.

Vonna, L., Wiedemann, A., Aepfelbacher, M. and Sackmann, E. (2007). Micromechanics of filopodia mediated capture of pathogens by macrophages. *Eur. Biophys. J.* **36**, 145-151.

Watarai, M., Funato, S. and Sasakawa, C. (1996). Interaction of Ipa proteins of Shigella flexneri with alpha5beta1 integrin promotes entry of the bacteria into mammalian cells. *J. Exp. Med.* **183**, 991-999.

Young, V. B., Falkow, S. and Schoolnik, G. K. (1992). The invasin protein of Yersinia enterocolitica: internalization of invasin-bearing bacteria by eukaryotic cells is associated with reorganization of the cytoskeleton. *J. Cell Biol.* **116**, 197-207.